

# Reproducibility of SPECT Measurement of Benzodiazepine Receptors in Human Brain with Iodine-123-Iomazenil

Anissa Abi-Dargham, Mitchell Gandelman, Sami S. Zoghbi, Marc Laruelle, Ronald M. Baldwin, Penny Randall, Yolanda Zea-Ponce, Dennis S. Charney, Paul B. Hoffer and Robert B. Innis

*Departments of Psychiatry and Diagnostic Radiology, Yale University School of Medicine, New Haven, Connecticut and West Haven VA Medical Center, West Haven, Connecticut*

Iodine-123-iomazenil is a SPECT radiotracer used to image and quantify benzodiazepine receptors. The reproducibility of the measurement of benzodiazepine receptors in human brain with [<sup>123</sup>I]iomazenil and SPECT was investigated with a test/retest paradigm. **Methods:** Six subjects underwent two experiments during a 1-wk interval. Iodine-123-iomazenil was injected as a single bolus (12 mCi). The time-activity curves of the tracer in the arterial plasma were measured and corrected for metabolites. Regional time-activity curves of five brain regions were measured with the CERASPECT camera for 145 min postinjection with serial 2-min acquisitions. Data were analyzed using three kinetic models that included a two-compartment model, an unconstrained three-compartment model and a three-compartment model with a constraint on the nondisplaceable compartment. **Results:** The results from the various analyses and fitting strategies were compared. The variability (average absolute difference between test and retest, expressed as a percentage of the mean of both measurements) was 10% to 17%, depending on the outcome measure and the fitting procedure. The most reproducible outcome measure was the regional tracer distribution volume relative to the total arterial concentration ( $V_T'$ ).  $V_T'$  showed an average regional variability of  $10\% \pm 2\%$ , with an intraclass correlation coefficient of 0.81. **Conclusion:** SPECT measurement of regional [<sup>123</sup>I]iomazenil  $V_T'$  is reproducible and reliable. The use of regional ratios results in a significant loss of information.

**Key Words:** SPECT; iodine-123-iomazenil; reproducibility; benzodiazepine receptor

**J Nucl Med 1995; 36:167-175**

**Q**uantification of central neuroreceptors with SPECT is a relatively recent development in the field of nuclear medicine. Over the last few years, several iodinated high affinity ligands have been introduced, enabling the visual-

ization with SPECT of receptors such as the muscarinic cholinergic receptors (1,2), the dopaminergic D<sub>2</sub> receptors (3-6), the dopaminergic and serotonergic transporters (7-9) and the benzodiazepine receptors (10). Given the lower cost and wider availability of SPECT compared to PET, SPECT may represent a viable alternative to PET for clinical investigations. Since SPECT has a lower sensitivity than PET, however, the accuracy and reproducibility of the quantification of receptors obtained with SPECT need to be evaluated.

Iomazenil is a benzodiazepine antagonist with a high affinity ( $K_D = 0.35$  nM at 22°C, 0.66 nM at 37°C) for the central type of benzodiazepine receptors (10). Labeled with <sup>123</sup>I, iomazenil has been used in nonhuman primates (11) and healthy human subjects (12) as a SPECT tracer with high specific brain uptake. Using both kinetic analysis of single bolus experiments (13) and equilibrium analysis of constant infusion experiments with high and low specific activity [<sup>123</sup>I]iomazenil (14), the in vivo benzodiazepine receptor density ( $B_{max}$ ) and affinity ( $1/K_D$ ) were measured with SPECT in several brain regions in baboons. These receptor parameters were measured in vitro in the same animals after sacrifice and were found to be in excellent agreement with the SPECT in vivo determination (14).

In humans, high specific activity experiments were performed to measure the benzodiazepine receptor binding potential (BP, equal to  $B_{max}/K_D$ ) with both kinetic and equilibrium paradigms (15). The distribution of [<sup>123</sup>I]iomazenil BP among brain regions was in accordance with the known distribution of benzodiazepine receptors in humans and the value of BP was in accordance with in vitro values measured in human cortical membranes. Altogether, these studies suggested that SPECT could be used for quantification of benzodiazepine receptor parameters in the living human brain.

The present study addresses the question of the reproducibility of SPECT [<sup>123</sup>I]iomazenil quantification of benzodiazepine receptors in humans. In baboons, the variability of SPECT measurement of BP using different modes of administration of the tracer and different methods of data

Received Feb. 17, 1994; revision accepted Aug. 1, 1994.

For correspondence and reprints contact: Anissa Abi-Dargham, MD, Department of Psychiatry, Yale University and West Haven VA Medical Center/116A2, 950 Campbell Avenue, West Haven, CT 06516.

analysis varied between 7% and 15% (13,14). Whether these results can be extended to humans is unclear. In humans, the activity distributes in a much larger body volume than in baboons, leading to lower levels of activity in brain and plasma. Head movement during data acquisition and limitations in the duration of the scanning constitute additional sources of noise in the human data. Therefore, it was important to study the reproducibility of the measurement in this apparently less favorable situation. In the design of clinical studies, such information is needed to select the most appropriate method of analysis and to incorporate the assay variability into the power analysis.

In the brain, the tracer distributes between the specific (receptor bound) and nondisplaceable (free and nonspecifically bound) compartments. The total equilibrium volume of distribution is the sum of the specific and nondisplaceable equilibrium volumes of distribution. The specific equilibrium volume of distribution is equal to BP when experiments are performed at tracer doses and when the equilibrium distribution volume is expressed relative to the free authentic arterial tracer concentration.

For [ $^{123}\text{I}$ ]iomazenil, the nondisplaceable compartment cannot be readily measured because of the absence of a region devoid of receptors. Fortunately, this compartment represents only 10% to 15% of the total volume of distribution in the cortex and can be neglected (15). In this situation, the total tissue volume of distribution is determined by the receptor density and can be used as a valid outcome measure (16). The kinetic analysis derives the equilibrium volume of distribution from the ratio of the rate constants characterizing the transfer of the tracer between the different compartments.

The purpose of this study was to measure the reproducibility of [ $^{123}\text{I}$ ]iomazenil equilibrium volumes of distribution derived from kinetic analyses of single bolus injections. We compared the reproducibility of three outcome measures derived from three fitting strategies: a two-compartment model, an unconstrained three-compartment model and a three-compartment model with a constraint on the value of the nondisplaceable compartment. In addition, we assessed the reproducibility of a relative measure of the regional distribution volumes obtained by calculating the ratio of the distribution volumes in several cortical regions to that in the occipital region. Because these ratios are not sensitive to errors in the cross calibration of brain and plasma activity, a better reproducibility would be expected compared to the absolute measurements of distribution volumes.

## METHODS

### Radlodeling

No carrier added to [ $^{123}\text{I}$ ]iomazenil was prepared by iododestannylation of ethyl 7-(tributylstannyl)-5,6-dihydro-5-methyl-6-oxo-4H-imidazo[1,5-a][1,4]benzodiazepine-3-carboxylate with chloramine-T in methanolic acetic acid at 120°C as previously described (15,17). The radiochemical yield of the preparations averaged 86.1%  $\pm$  5.2% (with these and subsequent data ex-

pressed as mean  $\pm$  SD,  $n = 12$ ) and the radiochemical purity averaged 96.9  $\pm$  2.4.

### Experimental Design

The study represents a set of 12 consecutive experiments carried out over a period of 6 mo. The average interval between a test and retest experiment was 8  $\pm$  2 days.

Six healthy subjects (age 28  $\pm$  9 yr, weight 86  $\pm$  15 kg, 5 males and 1 female) were recruited for these studies. Inclusion criteria were: absence of current medical conditions; absence of neuropsychiatric illnesses, alcohol or substance abuse; and no alcohol consumption for 2 wk prior to the first test and until completion of the retest. A physical examination, EKG and routine blood and urine tests were performed in the screening procedure. All subjects gave written informed consent. Subjects received potassium iodide (SSKI solution 0.6 g) in the 24 hr period prior to scan. All subjects enlisted in the study completed both test and retest experiments and, therefore, data from all subjects were included.

### Data Acquisition

Data were acquired as previously described (15). Four fiducial markers filled with 10  $\mu\text{Ci}$  of [ $^{99\text{m}}\text{Tc}$ ]NaTcO<sub>4</sub> were attached on both sides of the subject's head at the level of the cantho-meatal line to control for positioning of the head in the gantry before tracer injection and to identify the cantho-meatal plane during image analysis. Efforts were made to place the fiducial markers in a reproducible manner, following anatomically defined criteria. An indwelling catheter was inserted in the radial artery. Iodine-123-iomazenil (12.1  $\pm$  0.4 mCi) was intravenously injected as a single bolus over 30 sec. SPECT data were acquired with the multislice brain-dedicated CERASPECT camera (Digital Scintigraphics, Waltham, MA; 17). Scans were acquired in continuous mode every 2 min for 145  $\pm$  5 min. Arterial blood samples (1 to 2 ml) were collected every 20 sec for the first 2 min with a peristaltic pump (Harvard 2501-001, South Natick, MA) and then manually at 3, 4, 6, 8, 12, 16, 20, 30, 45 and 60 min. After the first hour, samples were drawn every 30 min until the end of the experiment.

### Image Analysis

Images were reconstructed from counts acquired in the  $^{123}\text{I}$  photopeak (159 keV) with a 20% symmetric window using a Butterworth filter (cutoff = 1 cm, power factor = 10) and displayed on a 64  $\times$  64  $\times$  32 matrix (pixel size = 3.3 mm  $\times$  3.3 mm, slice thickness = 3.3 mm, voxel volume = 36.7 mm<sup>3</sup>). Attenuation correction was performed assuming uniform attenuation equal to that of water (attenuation coefficient  $\mu = 0.150 \text{ cm}^2/\text{g}$ ) within an ellipse drawn around the skull as identified by the markers. Images were reoriented so that the cantho-meatal plane, identified by the four fiducial markers, corresponded to the transaxial plane of the data set.

The level of highest occipital concentration was identified by inspection of the 32 images of an acquisition obtained after peak brain uptake, usually 30 min postinjection. This level was invariably located 9 to 10 slices above the cantho-meatal plane. A set of 8 slices including 4 images below and 3 above the level of maximal occipital activity were then summed (upper slice). Three slices were summed at the level of the cantho-meatal plane as defined by the markers (lower slice). Five ROIs were analyzed. A cerebellar ROI (4.4 cm<sup>2</sup>) was positioned on the lower slice. Occipital (4.0 cm<sup>2</sup>), temporal (3.3 cm<sup>2</sup>), cingulate (1.2 cm<sup>2</sup>) and frontal (2 cm<sup>2</sup>) ROIs were positioned on the upper slice. No attempts were made to correct for the scatter fraction within the photopeak window nor for partial voluming effects.

Average cpm/pixel ROI activities were measured, decay corrected for the time of injection, and expressed in  $\mu\text{Ci}/\text{cm}^3$  using a calibration factor of  $0.0046 \mu\text{Ci}/\text{cpm}$ . This value was the average calibration factor obtained from eight phantom experiments performed at regular intervals during the period of the study. An  $^{123}\text{I}$  distributed source of 13.5 cm diameter ( $4.7 \pm 0.8 \mu\text{Ci}/\text{ml}$ ) was acquired for 10 min and reconstructed using the same protocol used in the study. The average cpm/cm<sup>3</sup> was measured in a large ROI (7.7 cm<sup>2</sup>) positioned in the middle of the phantom image. Aliquots of the phantom solution ( $n = 10$ ) were measured on the gamma counter (1282 Compugamma Cs, Wallac Inc., Turku, Finland) used for measuring the plasma activity. The calibration factor ( $0.0046 \pm 0.0007 \mu\text{Ci}/\text{cpm}$ ) was calculated as the ratio of the image cpm/cm<sup>3</sup> to the solution activity ( $\mu\text{Ci}/\text{ml}$ ). Measurement of the calibration factor showed random noise with no evidence of consistent change over time. This calibration factor is lower than the one used in our previous study, which was derived from one single phantom experiment. Therefore, distribution volumes reported here are lower than previously reported (15).

### Arterial Plasma Analysis

Blood samples were analyzed as previously described (18). Extraction (ethyl acetate) was followed by reverse-phase HPLC to measure the metabolite-corrected total plasma activity ( $\text{Ca}(t)$ ,  $\mu\text{Ci}/\text{ml}$ ). Measured metabolite-corrected total plasma activity data were fit to a sum of three exponentials and the clearance ( $C_L$ , liter/hr) was calculated as previously described (15).

The free fraction of plasma parent compound ( $f_1 = \text{free parent}/\text{Ca}(t)$ ) was measured in each subject by ultrafiltration with Centrifree micropartition system (Amicon Division, W.R. Grace & Co., Danvers, MA). The method for calculating  $f_1$  was different from the method used in the previous study (15). Two improvements were implemented in this study.

First, the new method (19) derives the free fraction as the ratio of the ultrafiltrate concentration to the plasma concentration. In the previously used method, the free fraction was measured as the ratio of the ultrafiltrate to the total activity in the assay tube, including the ultrafiltrate and the activity bound to the filter. Because of free tracer retention on the filter, the previous method underestimated the free fraction. Therefore, the BP values reported in this study are not directly comparable to the BP values previously published.

Second, a standard sample, made of pooled frozen human plasma, was processed with each assay to control for the inter-assay variability. For each study, two aliquots of this standard were thawed, [ $^{123}\text{I}$ ]iomazenil was added and the  $f_1$  was measured at the same time and in an identical manner to the plasma samples acquired in the scanning session. The free fraction of this standard was measured for each of the twelve experiments and showed no evidence of consistent change over time. Individual experimental  $f_1$  values were corrected by multiplying by the average  $f_1$  of the standard ( $0.39 \pm 0.02$ ) divided by the value of the standard measured in that individual study.

### Derivation of Receptor Parameters

Kinetic analyses were performed using a two- and a three-compartment model analysis as previously described (13,15). The two-compartment model consists of an arterial compartment ( $C_a$ ) and a brain compartment ( $C_T$ ), the latter of which includes free, nonspecifically bound, and specifically bound tracer. The three-compartment model consists of the arterial compartment ( $C_a$ ), the nondisplaceable compartment ( $C_2$ ; free and nonspecifically bound tracer) and the receptor compartment ( $C_3$ ).

The equilibrium volume of distribution of a compartment  $i$  relative to the free tracer ( $V_i$ ,  $\text{ml g}^{-1}$ ) was defined as the equilibrium ratio of the tracer concentration in compartment  $i$  to the free tracer concentration in the arterial plasma,

$$V_i = \frac{C_i}{f_1 C_a} \quad \text{Eq. 1}$$

Thus  $V_2$ ,  $V_3$  and  $V_T$  are the nondisplaceable, specific and total equilibrium distribution volumes, respectively, relative to the free arterial tracer concentration. Since all experiments were performed at tracer doses, the equilibrium distribution volume of the receptor compartment,  $V_3$ , was equal to BP (14).

Similarly, the equilibrium volume of distribution of a compartment  $i$  relative to the total tracer ( $V'_i$ ,  $\text{ml g}^{-1}$ ) was defined as the equilibrium ratio of the tracer concentration in compartment  $i$  to the total tracer concentration in the arterial plasma,

$$V'_i = \frac{C_i}{C_a} \quad \text{Eq. 2}$$

from which it follows that  $V'_i = V_i/f_1$ . Thus  $V'_2$ ,  $V'_3$ , and  $V'_T$  are the nondisplaceable, specific and total equilibrium distribution volumes, respectively, relative to the total arterial tracer concentration.

The two-compartment model used two rate constants,  $K_1$  ( $\text{ml g}^{-1} \text{min}^{-1}$ ) and  $k'_2$  ( $\text{min}^{-1}$ ), describing the transfer of the tracer in and out of the brain. The three-compartment model used four rate constants:  $K_1$  ( $\text{ml g}^{-1} \text{min}^{-1}$ ) and  $k_2$  ( $\text{min}^{-1}$ ), the forward and reverse transfer rate constants across the blood brain barrier;  $k_3$  ( $\text{min}^{-1}$ ) and  $k_4$  ( $\text{min}^{-1}$ ), the receptor-ligand association and dissociation rate constants. Rate constants were estimated by nonlinear regression using a Levenberg-Marquart least squares minimization procedure (20) implemented in MATLAB (The Math Works, Inc., South Natick, MA) on a Macintosh Quadra 950 as previously described (13).

Equilibrium distribution volumes were calculated from the ratios of the rate constants (13).

In the two-compartment model,

$$V_T = K_1/(k'_2 f_1) \quad \text{Eq. 3}$$

In the three-compartment model,

$$\begin{aligned} V_2 &= K_1/(k_2 f_1), \\ V_3 &= (K_1 k_3)/(k_2 k_4 f_1) = \text{BP}, \end{aligned} \quad \text{Eq. 4}$$

$$V_T = V_2 + V_3 = \frac{K_1(1 + k_3/k_4)}{k_2 f_1}.$$

Constraining the value of  $V_2$  has been shown to increase the accuracy and reproducibility of BP (13). Two fitting strategies (unconstrained and constrained) were therefore implemented for the three-compartment model. In the constrained fit, the  $K_1/k_2$  ratio was constrained to 3.2. This constraint was based on results from previously acquired data in humans using injections of receptor saturating doses of flumazenil (0.2 mg/kg) in bolus plus constant infusion experiments to determine the nondisplaceable compartment (15). In these experiments, we did not observe any significant differences between regions in the nonspecific volume of distribution. Therefore, the same constraint was used for all regions.

Goodness of fit of the two- and three-compartment models,

constrained and unconstrained fits, was compared using the Akaike criteria and the F-test as previously described (13).

In addition to absolute measurements of distribution volumes, the reproducibility of regional ratios of distribution volumes was also examined. Regional ratios can be useful for detecting selective regional alterations in benzodiazepine receptors such as in temporal lobe epilepsy. Because of the absence of measurable region of interest (ROI) devoid of receptors, we arbitrarily chose the occipital as the reference region for these ratios.

### Statistical Analysis

The variability of one measurement between test and retest was computed as the absolute value of the difference between test and retest, expressed in percentage of the mean value of both measurements. Differences in variability between different outcome measures or different fitting strategies were investigated by a repeated measure ANOVA with the region as cofactor.

The reproducibility of the measurements was further assessed relatively to the between subjects variance by the intraclass correlation coefficient,  $\rho$ , calculated as (21):

$$\frac{\text{MSBS} - \text{MSWS}}{\text{MSBS} + (n - 1) \text{MSWS}}, \quad \text{Eq. 5}$$

where MSBS is the mean sum of square between subjects and MSWS is the mean sum of square within subjects. This coefficient estimates the reliability of the measurement and can vary between 0 (no reliability) and 1 (maximum reliability, achieved in case of identity between test and retest, i.e. MSWS = 0).

## RESULTS

### Plasma Analysis

The mean clearance of the arterial parent compound was  $133 \pm 23$  liter/hr (Table 1, Fig. 1). Average percent change between test and retest was  $10.8\% \pm 10.8\%$ , with  $\rho = 0.76$ . The variability of  $f_1$  was  $10.8 \pm 8.0\%$  before correction for the between assay variability. When  $f_1$  measurements were corrected using the standard sample, the variability improved to  $6.5\% \pm 5.2\%$ . The average standard corrected  $f_1$  value was  $0.33 \pm 0.02$ , a value larger than previously measured in humans with the previous method ( $0.23 \pm 0.02$ ,  $n = 6$ , (15)). The  $f_1$  value showed little variation between subjects, ranging between 0.29 and 0.39, and the intraclass correlation was low ( $\rho = 0.43$ ).

### Brain Analysis

**Two-Compartment Model.** The fitting procedure converged in 71 out of 72 regressions (one cerebellar region failed to converge). Average values of  $V_T$  were: occipital,  $88 \pm 13$  ml  $g^{-1}$ ; frontal,  $76 \pm 15$  ml  $g^{-1}$ ; cingulate,  $80 \pm 16$  ml  $g^{-1}$ ; temporal,  $82 \pm 17$  ml  $g^{-1}$ ; cerebellum,  $45 \pm 13$  ml  $g^{-1}$ . The variability was considerable ( $17 \pm 2\%$ ) and the intraclass correlation was low ( $\rho = 0.50$ ; Table 2). Average values of  $V_T'$  were: occipital,  $29 \pm 4$  ml  $g^{-1}$ ; frontal,  $25 \pm 5$  ml  $g^{-1}$ ; cingulate,  $26 \pm 6$  ml  $g^{-1}$ ; temporal,  $27 \pm 7$  ml  $g^{-1}$ ; cerebellum,  $15 \pm 6$  ml  $g^{-1}$ . The variability was  $12 \pm 3\%$  with  $\rho = 0.75$ . The reproducibility of  $V_T'$  was significantly better than  $V_T$  ( $p < 0.005$ ).

**Three-Compartment Model, Unconstrained Fit.** The fitting procedure failed to converge in 2 out of the 72 regres-

**TABLE 1**  
Plasma Clearance and Free Fraction: Values, Variability and Reliability

Subject no.	Study	$C_L$ (liter/hr)	% Change	$f_1$	% Change
1	1	119		0.32	
	2	121	1.4%	0.30	6.2%
2	1	166		0.31	
	2	155	6.7%	0.33	3.9%
3	1	116		0.32	
	2	132	13.0%	0.31	1.6%
4	1	103		0.37	
	2	99	3.4%	0.33	9.9%
5	1	109		0.32	
	2	149	31.2%	0.33	2.3%
6	1	156		0.39	
	2	171	9.2%	0.34	15.3%
Average			10.8%		6.5%
s.d.			10.8%		5.2%
$\rho$			0.73		0.43

$C_L$  = plasma clearance of the parent compound, metabolites corrected;  $f_1$  = free fraction of the tracer in plasma, as measured in vitro by ultrafiltration, corrected for interassay variations; % change = absolute value of the test/retest difference, expressed as percentage of the mean of the test and retest;  $\rho$  = intraclass correlation coefficient.

sions (1 temporal and 1 cerebellar region). Estimates of  $V_T$  with the unconstrained three-compartment model were significantly higher than with the two-compartment model by  $9.5 \pm 8.6\%$  ( $p < 0.0005$ ). Mean regional  $V_T$  values were: occipital,  $93 \pm 12$  ml  $g^{-1}$ ; frontal,  $82 \pm 15$  ml  $g^{-1}$ ; cingulate,  $89 \pm 19$  ml  $g^{-1}$ ; temporal,  $93 \pm 18$  ml  $g^{-1}$ ; cerebellum,  $50 \pm 21$  ml  $g^{-1}$ . Mean regional variability was  $13 \pm 2\%$  with  $\rho = 0.61$  (Table 3). The reproducibility of  $V_T$  derived from the unconstrained three-compartment fit was statistically superior to the reproducibility of  $V_T$  derived from the two compartment fit ( $p < 0.05$ ). Mean regional  $V_T'$  values were: occipital,  $31 \pm 5$  ml  $g^{-1}$ ; frontal,  $27 \pm 6$  ml  $g^{-1}$ ; cingulate,  $29 \pm 8$  ml  $g^{-1}$ ; temporal,  $31 \pm 8$  ml  $g^{-1}$ ; cerebellum,  $14 \pm 2$  ml  $g^{-1}$ . Values of  $V_T'$  (Table 4) showed the lowest variability ( $10 \pm 2\%$ ) and highest reliability ( $\rho = 0.81$ ) of all outcome measures. Similarly to the two-compartment analysis,  $V_T'$  reproducibility was statistically superior to  $V_T$  ( $p < 0.01$ ). However, the mean regional variability of  $V_2'$  and  $V_3'$  by the unconstrained three-compartment fit was  $14 \pm 2\%$  and  $17 \pm 2\%$ , respectively.

**Three-Compartment Model, Constrained Fit.** Values of rate constants and outcome measures for the occipital cortex are listed in Table 5. Average values of  $V_T'$  were: occipital,  $30 \pm 4$  ml  $g^{-1}$ ; frontal,  $27 \pm 5$  ml  $g^{-1}$ ; cingulate,  $28 \pm 6$  ml  $g^{-1}$ ; temporal,  $28 \pm 6$  ml  $g^{-1}$ ; cerebellum,  $14 \pm 1$  ml  $g^{-1}$ . The overall variability of  $V_T'$  was  $12 \pm 2\%$  ( $\rho = 0.72$ ), which was not statistically different from the variability of  $V_T'$  by the unconstrained fit ( $p = 0.11$ ; Table 6).

Average regional values of  $V_2'$  were: occipital,  $27 \pm 4$  ml  $g^{-1}$ ; frontal,  $23 \pm 5$  ml  $g^{-1}$ ; cingulate,  $25 \pm 6$  ml  $g^{-1}$ ; temporal,  $25 \pm 6$  ml  $g^{-1}$ ; cerebellum,  $12 \pm 1$  ml  $g^{-1}$ . The

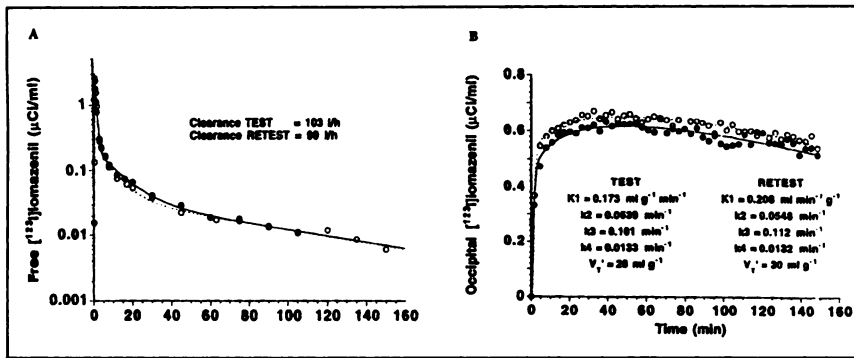


**FIGURE 1.** Time-activity curves of plasma-free [<sup>123</sup>I]iomazenil (A) and occipital [<sup>123</sup>I]iomazenil (B) after bolus injections of 12.1 mCi in Subject 4. Circles are measured values and lines are fitted values for the test (closed circles and solid lines) and the retest (open circles and dotted lines) experiments. Data were fitted to a three exponential model for the plasma activity and a constrained three-compartment model for the occipital activity. Values of the clearance and occipital distribution volume ( $V_T'$ ) were derived from the regressions as explained in the method section. In this subject, the variability of the clearance and  $V_T'$  were 3.4% and 10%, respectively.

variability of  $V_3'$  ( $14 \pm 2\%$ ,  $\rho = 0.72$ ; Table 6) was statistically improved with the constrained fit as compared to the unconstrained fit ( $p < 0.0005$ ).

### Goodness of Fit

Between fit differences in Akaike criteria were compared for each region and each subject with a repeated measure ANOVA. In each region, with the exception of the cingulate, Akaike criteria for the three-compartment constrained fit was significantly lower than for the two-compartment fit ( $p < 0.01$  in all regions, except cingulate,  $p = 0.15$ ). In contrast, there were no significant differences between the Akaike values of the unconstrained and constrained three-compartment fit ( $p > 0.05$  in all regions). These results were confirmed by the F-test. In all subjects and all regions, the constrained three-compartment model produced a significant improvement of the fit as compared to the two-compartment model, while the unconstrained three-compartment fit produced significantly better fit than the constrained three-compartment fit in only 66% of the curves.

### Regional Ratios

Average values of frontal to occipital, cingulate to occipital and temporal to occipital distribution volume ratios

were  $0.88 \pm 0.10$ ,  $0.91 \pm 0.10$  and  $0.98 \pm 0.11$ . The variability of these ratios was lower than the variability of the measurement of the distribution volumes themselves:  $7.9 \pm 6.3\%$ ,  $7.8 \pm 6.5\%$  and  $5.4 \pm 61\%$  for the frontal, cingulate and temporal to occipital ratios, respectively. However, because of the large variation in variability, this improvement did not reach statistical significance ( $p = 0.09$ ). The intraclass correlation coefficients of the regional ratios were lower than of  $V_T'$ , with  $\rho$  values of 0.66, 0.65 and 0.74 for the frontal, cingulate, and temporal to occipital ratios, respectively.

### DISCUSSION

This study indicates that brain regional distribution volumes of [<sup>123</sup>I]iomazenil can be measured with SPECT and kinetic analysis with variability ranging from 10% to 17%, depending on the method of analysis and the choice of outcome measure. The regional distribution volume relative to the total arterial parent compound ( $V_T'$ ) derived from an unconstrained three-compartment model analysis was the most reproducible and reliable outcome measure (variability:  $10 \pm 2\%$ , reliability:  $\rho = 0.81$ ).

Attempts to control for the plasma protein binding of the

**TABLE 2**  
Two-Compartment Kinetic Analysis: Variability and Reliability (%)

Subject no.	Occipital		Frontal		Cingulate		Temporal		Cerebellar	
	$V_T$	$V_T'$	$V_T$	$V_T'$	$V_T$	$V_T'$	$V_T$	$V_T'$	$V_T$	$V_T'$
1	25	18	17	10	19	13	21	15	27	21
2	3	1	11	7	5	1	11	7	15	11
3	16	17	5	7	16	17	11	12	5	6
4	21	11	23	13	22	12	26	16	17	7
5	12	15	10	12	13	15	13	15	17	15
6	27	12	16	1	31	16	26	11	—	—
Mean $\pm$ s.d.	$17 \pm 9$	$12 \pm 6$	$14 \pm 6$	$8 \pm 4$	$18 \pm 9$	$13 \pm 6$	$18 \pm 7$	$13 \pm 3$	$16 \pm 8$	$12 \pm 6$
$\rho$	0.08	0.59	0.73	0.91	0.51	0.80	0.58	0.85	0.62	0.80

\*Values are test/retest variability (absolute value of the test/retest difference, expressed as percentage of the mean of the test and retest).

\*\*Cerebellar variability values are not provided for Subject 6 due to lack of convergence of retest experiment.

$V_T$  = regional tracer equilibrium distribution volume relative to the free arterial tracer;  $V_T'$  = regional tracer equilibrium distribution volume relative to the total arterial tracer;  $\rho$  = intraclass correlation coefficient.

**TABLE 3**  
Unconstrained Three-Compartment Kinetic Analysis: Values of  $V_T'$  (ml · g<sup>-1</sup>)

Subject no.	Experiment no.	Occipital	Frontal	Cingulate	Temporal	Cerebellar
1	1	28.6	23.9	23.4	25.2	12.9
	2	32.9	25.6	26.6	29.4	15.8
2	1	27.1	23.0	23.0	24.4	14.0
	2	26.8	20.5	22.0	22.7	12.9
3	1	27.9	23.8	27.7	26.3	12.8
	2	25.0	21.5	23.9	24.6	14.4
4	1	29.6	22.8	24.9	—	15.8
	2	30.2	28.0	28.8	26.2	15.3
5	1	28.9	29.7	30.6	30.4	14.9
	2	32.7	34.6	35.3	34.3	12.3
6	1	38.0	37.0	43.7	46.3	17.1
	2	40.8	36.9	43.2	42.6	—
Mean ± s.d.		30.7 ± 4.7	27.3 ± 6.0	29.4 ± 7.5	30.2 ± 7.8	14.4 ± 1.5

\*Values are  $V_T'$  (ml g<sup>-1</sup>) which is the regional tracer equilibrium distribution volume relative to the total arterial tracer.

\*\*The temporal and cerebellar time-activity curves failed to converge in Subject 4 test and Subject 6 retest.

tracer increased the noise of the measurement. Potential differences in plasma protein concentrations between subjects affect the free concentration of the tracer (13,22). We had predicted a priori that this potentially confounding factor should be controlled by expressing the distribution volume relative to the free parent compound ( $V_T$ ) rather than to the total parent compound ( $V_T'$ ). However, in this study, the additional noise introduced by this correction exceeded the potential increase in reproducibility. Although the in vitro measurement of  $f_1$  was achieved with acceptable variability (6.5%), all subjects showed similar levels of plasma protein binding, inducing a poor reliability ( $\rho = 0.46$ ). Although this study did not support the utility of this correction in healthy subjects, it may still be necessary to control for potential alterations of plasma protein binding in pathological conditions.

The variability of  $V_3'$  derived by the unconstrained fit (17%) was higher than the variability of  $V_T'$  (10%). The difficulties associated with the measurement of  $V_3'$  by an unconstrained three-compartment fit have been well documented (13,15,23,24) and derive from the lack of identifiability and high covariance of the individual rate constants. Constraining the value of  $V_2'$  to 3.2 decreased the variability of  $V_3'$  from 17% to 13%. This observation replicated a similar finding in baboons, in which a constraint on  $V_2'$  decreased the variability of  $V_3'$  from within 15% to 10% (13). This improvement confirmed the error introduced in  $V_3'$  by the limited ability of the regression procedure to identify the different components of  $V_T'$  ( $V_2'$  and  $V_3'$ ). The constraining procedure had minimal impact on the value of  $V_T'$  and did not significantly affect its reproducibility. Thus, in contrast with  $V_3'$ , the constrained and uncon-

**TABLE 4**  
Unconstrained Three-Compartment Kinetic Analysis: Variability and Reliability (%)

Subject no.	Occipital		Frontal		Cingulate		Temporal		Cerebellar	
	$V_T$	$V_T'$	$V_T$	$V_T'$	$V_T$	$V_T'$	$V_T$	$V_T'$	$V_T$	$V_T'$
1	20	14	13	7	19	13	21	15	12	20
2	5	1	15	11	8	4	11	7	14	8
3	9	11	9	10	13	15	5	7	16	12
4	12	2	30	20	24	14	—	—	4	3
5	10	12	13	15	12	14	10	12	14	19
6	23	7	15	0	14	1	7	8	—	—
Mean ± s.d.	13.1 ± 6.8	7.9 ± 5.5	15.8 ± 7.5	10.8 ± 6.9	15.0 ± 5.6	10.2 ± 5.9	10.9 ± 6.3	9.9 ± 3.7	11.8 ± 4.7	12.6 ± 7.3
$\rho$	0.31	0.83	0.63	0.86	0.74	0.92	0.84	0.93	0.51	0.53

\*Values are test/retest variability (absolute value of the test/retest difference, expressed as percentage of the mean of the test and retest).

\*\*The temporal and cerebellar time-activity curves failed to converge in Subject 4 test and Subject 6 retest, respectively.

$V_T$  = regional tracer equilibrium distribution volume relative to the free arterial tracer;  $V_T'$  = regional tracer equilibrium distribution volume relative to the total arterial tracer;  $\rho$  = intraclass correlation coefficient.

**TABLE 5**  
Constrained Three-Compartment Kinetic Analyses in the Occipital Region: Rate Constants and Distribution Volumes

Subject no.	Experiment no.	$K_1$ ml g <sup>-1</sup> min <sup>-1</sup>	$k_2$ min <sup>-1</sup>	$k_3$ min <sup>-1</sup>	$k_4$ min <sup>-1</sup>	$V_3$ ml g <sup>-1</sup>	$V_T'$ ml g <sup>-1</sup>
1	1	0.207	0.0644	0.124	0.0159	25	28
	2	0.225	0.0700	0.205	0.0224	29	33
2	1	0.182	0.0568	0.149	0.0201	24	27
	2	0.180	0.0561	0.159	0.0214	24	27
3	1	0.184	0.0572	0.136	0.0171	25	29
	2	0.183	0.0571	0.138	0.0214	21	24
4	1	0.173	0.0539	0.101	0.0133	24	28
	2	0.208	0.0648	0.112	0.0132	27	30
5	1	0.237	0.0738	0.174	0.0219	26	29
	2	0.317	0.0988	0.237	0.0257	30	33
6	1	0.242	0.0753	0.457	0.0484	30	33
	2	0.372	0.1159	0.145	0.0127	37	40
Mean ± s.d.		0.226 ± 0.061	0.070 ± 0.019	0.178 ± 0.096	0.0211 ± 0.0096	27 ± 4	30 ± 4

$K_1$ – $k_4$  = kinetic rate constants (see methods for definitions);  $V_3$  and  $V_T'$  = regional tracer distribution volume relative to the total arterial tracer of the specific, and total compartments.

strained fit were equivalent in the case of  $V_T'$ , which suggests that a constraining procedure is not needed for the derivation of  $V_T'$ .

Because of the relatively low contribution of  $V_2$  to  $V_T'$ ,  $V_T'$  is a reasonable outcome measure. In other terms,  $V_T'$  is mostly determined by  $V_3$  because  $V_2$  is negligible. The alternative is to measure  $V_2$  directly by displacement experiments (15), which may be indicated in the study of disease states where the contribution of  $V_2$  to  $V_T'$  is different than in healthy controls.

If  $V_T$  is elected as outcome measure, the evaluation of a two-compartment model appears warranted because of its computational facility. This approach has been implemented successfully with [<sup>11</sup>C]flumazenil (16). We have previously shown in baboons that a two-compartment model resulted in a significantly lower goodness of fit than a three-compartment model (13), which resulted in significant underestimation and lower reproducibility of  $V_T'$ .

This finding has been replicated in the present study. The two-compartment model does not appear as the model of choice for kinetic analysis of [<sup>123</sup>I]iomazenil uptake in humans. The higher affinity of iomazenil compared to flumazenil, leading to prolonged brain retention, might explain the differences in the performance of the two-compartment model between the two ligands.

Data concerning reproducibility of measurement of tracer brain uptake with PET have emerged only recently in the literature. The reproducibility of [<sup>11</sup>C]flumazenil has been studied in a test/retest paradigm where both studies are performed on the same day (25). The test and retest variability of regional distribution volume (DV, a measure equivalent to  $V_T'$  in our notation) ranged from –3.4% in the occipital cortex to –9.8% in the pons. Volkow et al. (26) reported the reproducibility of measurement of  $D_2$  receptors with [<sup>11</sup>C]raclopride. Applying the same analysis used in the present paper to these data, the variability was

**TABLE 6**  
Constrained Three-Compartment Kinetic Analysis: Variability and Reliability (%)

Subject no.	Occipital		Frontal		Cingulate		Temporal		Cerebellar	
	$V_3$	$V_T'$	$V_3$	$V_T'$	$V_3$	$V_T'$	$V_3$	$V_T'$	$V_3$	$V_T'$
1	16	15	9	7	13	11	14	12	24	19
2	0	0	4	4	1	1	2	2	11	8
3	21	18	17	14	28	24	14	12	1	1
4	11	10	17	15	17	15	23	20	3	3
5	15	13	16	15	17	15	13	12	28	22
6	19	17	0	0	23	21	17	16	—	—
Mean ± s.d.	13.7 ± 7.5	12.2 ± 6.6	10.5 ± 7.3	9.2 ± 6.4	16.5 ± 9.2	14.5 ± 8.1	13.8 ± 6.9	12.3 ± 6.0	13.4 ± 12.2	10.6 ± 9.4
$\rho$	0.51	0.51	0.85	0.85	0.69	0.69	0.80	0.80	0.75	0.75

\*Values are test/retest variability (absolute value of the test/retest difference, expressed as percentage of the mean of the test and retest).

\*\*The cerebellar time-activity curve failed to converge in Subject 6 retest.

$V_3$  and  $V_T'$  = regional tracer distribution volume relative to the total arterial tracer of the specific and total compartments, respectively.  $\rho$  = intraclass correlation coefficient.

5.4% for the striatal distribution volume (DV, a measure equivalent to  $V_T'$  in our notation) and 5.2% for the ratio striatal DV/cerebellar DV with  $\rho = 0.85$  ( $n = 5$ ). The higher reproducibility of these two studies may be due to the higher sensitivity of PET over SPECT. However, the rapid decay of  $^{11}\text{C}$  allowed repeating [ $^{11}\text{C}$ ]flumazenil and [ $^{11}\text{C}$ ]raclopride scans within 24 hr, as opposed to 8 days in the present study.

Vingerhoets et al. (27) reported the reproducibility of the measurement of the [ $^{18}\text{F}$ ]fluorodopa striatal uptake rate constant ( $K_i$ ) in healthy subjects scanned at 1–2 wk intervals. The within subject standard deviation varied from 8% to 10% of the mean and  $\rho$  varied between 0.80 and 0.91, depending on the size of the ROI. Thus, these results are comparable to the results of the present study. To our knowledge, the reproducibility of the  $f_1$  measurement has not been addressed in the PET literature.

The reproducibility of the regional ratios was better than the reproducibility of the absolute measurements. This higher reproducibility was expected, since ratio methods are not vulnerable to variations in the calibration of the counting devices or to error in the measurement of the input function. However, the reliability of the ratios was lower than that of the absolute measurements. The lower reliability implies that significant information pertaining to between subject differences is lost in the ratio methods. Similar conclusions were presented by Vingerhoets et al. (27), who compared the reliability of the  $K_i$  for [ $^{18}\text{F}$ ]fluorodopa with the ratio of striatal to occipital activity. In conclusion, ratio methods, at least in the experimental conditions of the present study, result in a significant loss of information compared to absolute quantification methods. Absolute quantification is thus preferable despite the additional cost in reproducibility.

The reproducibility of the scan reorientation according to the fiducial markers and that of the ROI placement on the SPECT image were not formally assessed in this study. These factors are likely to be major sources of variability between test and retest and could be improved by coregistering both SPECT studies to an MRI study. The MRI can be used to draw the ROIs, which can then be transferred to the SPECT images. This technique should increase the accuracy of the regional measurements and allow reproducible quantification of receptors in more discrete areas than used in the present studies. We are currently evaluating the improvement in reproducibility associated with MRI coregistration.

These test/retest studies represent the first attempt to evaluate the reproducibility of SPECT model-based measurements of neurotransmitter receptors and demonstrate that  $V_T'$  (tissue volume of distribution relative to the total arterial tracer) is a reproducible and reliable outcome measure.

#### ACKNOWLEDGMENTS

The authors thank W. Hunkeler, PhD, Hoffman-La Roche (Basle, Switzerland) for samples of iomazenil; and E.O. Smith,

G. Wisniewski, L. Pantages-Torok and Q. Ramsby for excellent technical assistance. This work was supported in part by funds from the National Alliance for Research on Schizophrenia and Depression, the Department of Veterans Affairs (Schizophrenia Research Center and the Center for the Study of Post-traumatic Stress Disorder) and the Public Health Service.

#### REFERENCES

- Mueller-Gartner H, Wilson A, Dannals R, Wagner H, Frost J. Imaging muscarinic receptors in human brain in vivo with SPECT, [ $^{123}\text{I}$ ]4-iododexetimide, and [ $^{123}\text{I}$ ]4-iodolevetimide. *J Cereb Blood Flow Metab* 1992;12:562–570.
- Gibson RE, Weckstein DJ, Jagoda EM, Rzeszutowski WJ, Reba RC, Eckelman WC. The characteristic of I-125 4-IQNB and H-3 QNB in vivo and in vitro. *J Nucl Med* 1984;25:214–222.
- Kung HF, Guo Y-Z, Billings J, et al. Preparation and biodistribution of [ $^{125}\text{I}$ ]IBZM: a potential CNS D2 dopamine receptor imaging agent. *Nucl Med Biol* 1988;15:195–201.
- Kung M-P, Kung HF, Billings J, Yang Y, Murphy RA, Alavi A. The characterization of IBF as a new selective dopamine D2 receptor imaging agent. *J Nucl Med* 1990;31:648–654.
- Kessler RM, Ansari MS, de Paulis T, et al. High affinity dopamine D2 receptor radioligands. I. Regional rat brain distribution of iodinated benzamides. *J Nucl Med* 1991;32:1593–1600.
- Hall H, Hogberg T, Halldin C, et al. NCQ 298, a new selective iodinated salicylamide ligand for the labeling of dopamine D2 receptors. *Psychopharmacology* 1991;103:6–18.
- Neumeyer JL, Wang S, Milius RA, et al. [ $^{123}\text{I}$ ]2 $\beta$ -carbomethoxy-3 $\beta$ -(4-iodophenyl)tropane ( $\beta$ -CIT): high affinity SPECT radiotracer of monoamine reuptake sites in brain. *J Med Chem* 1991;34:3144–3146.
- Carroll FI, Rahman MA, Abraham P, et al. [ $^{125}\text{I}$ ]3 $\beta$ -(4-iodophenyl)tropan-2 $\beta$ -carboxylic acid methyl ester (RTI-55), a unique cocaine receptor ligand for imaging the dopamine and serotonin transporters in vivo. *Med Chem Res* 1991;1:289–294.
- Mathis CA, Biegon A, Taylor SE, Enas JE, Hanrahan SM. [ $^{125}\text{I}$ ]5-Iodo-6-nitro-2-piperazinylquinoline: a potent and selective ligand for the serotonin uptake complex. *Eur J Pharmacol* 1992;210:103–104.
- Beer H-F, Blauenstein PA, Hasler PH, et al. In vitro and in vivo evaluation of iodine-123 Ro 16-0154: a new imaging agent for SPECT investigations of benzodiazepine receptors. *J Nucl Med* 1990;31:1007–1014.
- Innis RB, Zoghbi SS, Johnson EW, et al. SPECT imaging of the benzodiazepine receptor in non-human primate brain with [ $^{125}\text{I}$ ]Ro 16-0154. *Eur J Pharmacol* 1991;193:249–252.
- Woods SW, Seibyl JP, Goddard AW, et al. Dynamic SPECT imaging after injection of the benzodiazepine receptor ligand [ $^{125}\text{I}$ ]iomazenil in healthy human subjects. *Psych Res Neuroimaging* 1992;45:67–77.
- Laruelle M, Baldwin RM, Rattner Z, et al. SPECT quantification of [ $^{125}\text{I}$ ]iomazenil binding to benzodiazepine receptors in nonhuman primates. I. Kinetic modeling of single bolus experiments. *J Cereb Blood Flow Metab* 1994;14:439–452.
- Laruelle M, Abi-Dargham A, Al-Tikriti MS, et al. SPECT quantification of [ $^{125}\text{I}$ ]iomazenil binding to benzodiazepine receptors in nonhuman primates. II. Equilibrium analysis of constant infusion experiments and correlation with in vitro parameters. *J Cereb Blood Flow Metab* 1994;14:453–465.
- Abi-Dargham A, Laruelle M, Seibyl J, et al. SPECT measurement of benzodiazepine receptors in human brain with [ $^{125}\text{I}$ ]iomazenil: kinetic and equilibrium paradigms. *J Nucl Med* 1994;35:228–238.
- Koeppel RA, Holthoff VA, Frey KA, Kilbourn MR, Kuhl DE. Compartmental analysis of [ $^{11}\text{C}$ ]flumazenil kinetics for the estimation of ligand transport rate and receptor distribution using positron emission tomography. *J Cereb Blood Flow Metab* 1991;11:735–744.
- Zea-Ponce Y, Baldwin R, Zoghbi SS, Innis RB. Formation of 1- $^{125}\text{I}$ iodobutane in iododestannylation with [ $^{125}\text{I}$ ]iomazenil: implication for the reaction mechanism. *Int J Appl Radiat Isot* 1993;45:63–68.
- Zoghbi SS, Baldwin RM, Seibyl JP, et al. Pharmacokinetics of the SPECT benzodiazepine receptor radioligand [ $^{125}\text{I}$ ]iomazenil in human and nonhuman primates. *Nucl Med Biol* 1992;19:881–888.
- Gandelman MS, Baldwin RM, Zoghbi SS, Zea-Ponce Y, Innis RB. Evaluation of ultrafiltration for the free-fraction determination of single photon emission computed tomography (SPECT) radiotracers:  $\beta$ -CIT, IBF and iomazenil. *J Pharm Sci* 1994;83:1014–1019.
- Levenberg K. A method for the solution of certain problems in least squares. *Quart Appl Math* 1944;2:164–168.



21. Kirk RE. Experimental design: procedures for the behavioral sciences. 1982, Pacific Grove, California: Brooks & Cole Co.
22. Dubey RK, McAllister CB, Inoue M, Wilkinson GR. Plasma binding and transport of diazepam across the blood-brain barrier. No evidence for in vivo enhanced dissociation. *J Clin Invest* 1989;84:1155-1159.
23. Frost JJ, Douglass KH, Mayberg HS, et al. Multicompartmental analysis of <sup>11</sup>C-carfentanil binding to opiate receptors in human measured by positron emission tomography. *J Cereb Blood Flow Metab* 1989;9:398-409.
24. Price JC, Mayberg HS, Dannals RF, et al. Measurement of benzodiazepine receptor number and affinity in humans using tracer kinetic modeling, positron emission tomography, and [<sup>11</sup>C]-flumazenil. *J Cereb Blood Flow Metab* 1993;13:656-667.
25. Holthoff VA, Koepp RA, Frey KA, Kilbourn MR, Kuhl DE. Differentiation of radioligand delivery and binding in the brain: validation of a two-compartment model for [<sup>11</sup>C]flumazenil. *J Cereb Blood Flow Metab* 1991; 11:745-752.
26. Volkow ND, Fowler JS, Wang GJ, et al. Reproducibility of repeated measures of carbon-11-raclopride binding in the human brain. *J Nucl Med* 1993;34:609-613.
27. Vingerhoets FJG, Snow BJ, Schulzer M, et al. Reproducibility of fluorine-18-fluorodopa positron emission tomography in normal human subjects. *J Nucl Med* 1994;35:18-24.